Comment on "New Insights in the Electrocatalytic Proton Reduction and Hydrogen Oxidation by Bioinspired Catalysts: A DFT Investigation"

ARTICLE *in* THE JOURNAL OF PHYSICAL CHEMISTRY A · MAY 2011

Impact Factor: 2.69 · DOI: 10.1021/jp111479z · Source: PubMed

THE JOURNAL OF PHYSICAL CHEMISTRY A

COMMENT

pubs.acs.org/JPCA

Comment on "New Insights in the Electrocatalytic Proton Reduction and Hydrogen Oxidation by Bioinspired Catalysts: A DFT Investigation"

Michel Dupuis,* Shentan Chen, Simone Raugei, Daniel L. DuBois, and R. Morris Bullock

Center for Molecular Electrocatalysis, Chemical and Materials Sciences Division, Pacific Northwest National Laboratory, Richland, Washington, 99352, United States

Supporting Information

ABSTRACT: In the title paper, Vetere et al. reported a computational investigation of the mechanism of H_2 oxidation/proton reduction using a model of nickel-based electrocatalysts that incorporates pendant amines in cyclic phosphorus ligands. These catalysts are attracting considerable attention owing to their high turnover rates and relatively low overpotentials. These authors interpreted the results of their calculations as evidence for a symmetric bond cleavage of H_2 leading directly to two protonated amines in concert with a two-electron reduction of the Ni(II) site to form a Ni(0) diproton state. Proton reduction would involve a reverse symmetric bond formation. We report here an analysis that refutes the interpretation by these authors. We give, for the same model system, the structure of a heterolytic cleavage transition state consistent with the presence of the Ni(II) center acting as a Lewis acid and the pendant amines acting as Lewis bases. We present the associated intrinsic reaction coordinate (IRC) pathway connecting the dihydrogen (η^2-H_2) adduct and a hydride−proton state. We report also the transition state and associated IRC for the proton rearrangement from a hydride−proton state to a diproton state. Finally, we complete the characterization of the transition state reported by Vetere et al. through a determination of the corresponding IRC. In summary, H_2 oxidation/proton reduction with this class of catalysts involves a heterolytic bond breaking/formation.

INTRODUCTION

There is great current interest in catalysts that utilize inexpensive and abundant metals[1] for the interconversion of electrical and chemical energy, such as in the electrochemical oxidation and production of H_2 and reduction of O_2. In this context, the synthesis of highly efficient electrocatalysts for both hydrogen production and hydrogen oxidation has recently been reported.[2,3] These catalysts are mononuclear Ni(II) complexes containing cyclic diphosphine ligands with amine bases incorporated into the ligands. Their structure is depicted in I, and they are referred to as $Ni(P_2N_2)_2^{2+}$ complexes.

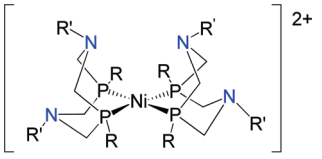

I

A key requirement for designing catalysts with enhanced efficiency is to obtain a detailed molecular-level understanding of the energetic and mechanistic factors controlling the activity of existing catalysts. Important insights have been derived from the early experimental work of Wilson et al.[4,5] and, more recently, those of Yang et al.[6,7] The presence and positioning of the amine bases near the metal center have been shown to be the most essential structural features contributing to the efficiency of these catalysts as the bases facilitate the heterolytic cleavage or formation of the H−H bond while acting as proton relays in the management of the proton and electron movement during the catalytic cycle.

Wilson et al.[4] put forth a description of the H_2 oxidation reaction mechanism in a closely related $Ni(PNP)_2^{2+}$ complex. The suggested pathway involved a rate-limiting heterolytic (asymmetric) transition state connecting a dihydrogen adduct at the nickel(II) center to a postulated hydride−proton intermediate, although the IRC pathway was not reported in that work. In ref 5, Wilson et al. suggested a different mechanism in a $Ni(P_2N_2)_2^{2+}$ catalyst involving symmetric cleavage of H_2 in concert with the transfer of the pair of electrons from the H_2 moiety to the Ni(II) center, although no spectroscopic evidence was reported establishing the nature of the transition state and no transition state for symmetric cleavage of H_2 was characterized computationally. We note that a heterolytic transition state had already been computed for R=R′=H in that paper. For a different complex that passes through a dihydride species, Yang et al.[6] suggested that transfer of a proton from the nickel to a pendant amine is a facile process. The recent work of Yang et al.,[7] along with some very recent theoretical work by Chen et al.[8] on a $Ni(P_2N_2)_2^{2+}$ complex, corroborated the proposal by Wilson et al.[4] of heterolytic H_2 cleavage followed by transfer of the proton from the nickel to a second pendant amine, forming a diproton Ni(0) state.

In a recently published paper,[9] Vetere et al. described the mechanism of H_2 evolution for the same class of $Ni(P_2N_2)_2^{2+}$

Received: December 2, 2010
Revised: February 18, 2011
Published: April 19, 2011

electrocatalysts as involving (i) direct H_2 bond formation starting from a diproton species via a symmetric transition state in concert with two-electron oxidation of the Ni(0) site to Ni(II) and (ii) the displacement of a dihydrogen adduct by an acetonitrile ligand to evolve H_2. The mechanistic character of the reaction or of its reverse reaction, whether it involves heterolytic cleavage or direct symmetric cleavage concerted with reduction, is of great interest as it has implications on the rational design of catalysts with enhanced activity and reduced overpotential.

An indication that the interpretation by Vetere et al.[9] of their calculations might be erroneous could be readily seen in Table 2 of their paper, showing the structure of the transition state with a H−H distance shorter, even if only slightly so, than in the H_2 adduct species (0.78 and 0.79 Å respectively) and much shorter than in a Ni-hydride/N-proton state (1.78 Å). The reported distance is only slightly longer than that in an isolated H_2 molecule. These authors state, "It seems that protons have completely migrated from the two N atoms to the Ni and that the H−H molecule is mostly formed". They report an imaginary frequency in the transition state of 406i cm^{-1}. They go on to acknowledge, "We have tried to link such a structure via an IRC analysis; nevertheless we could not achieve convergence of the pathway".

In what follows, we report calculations on the very same model system as Vetere's using a similar (although not precisely identical) computational methodology as theirs (see Computational Details). We determined the structure of a Ni-hydride/N-proton species (hydride−proton in short), a transition state that connects the hydride−proton state to a N-diproton state (diproton in short), and a heterolytic transition state that connects the hydride−proton species to a dihydrogen adduct. We generated all of the IRCs for these elementary steps. We determined the "Vetere" transition state and its associated IRC and analyzed the pathway as corresponding to a rotation (spinning) of the H_2 molecule in the dihydrogen adduct along the axis passing through the nickel atom and bisecting the H_2 molecule in its local minimum-energy conformation. This IRC does not connect the diproton state to the H_2-adduct state to H_2 evolution. In the H_2-adduct state, the H_2 molecule is weakly bound to the Ni(II) complex. Its barrier to rotation is low, and in fact, it is lower than the barrier to heterolytic cleavage. Nevertheless, the reactive mechanism of H−H formation starting from the diproton species involves multiple intermediates and multiple steps, the key one being heterolytic bond making.

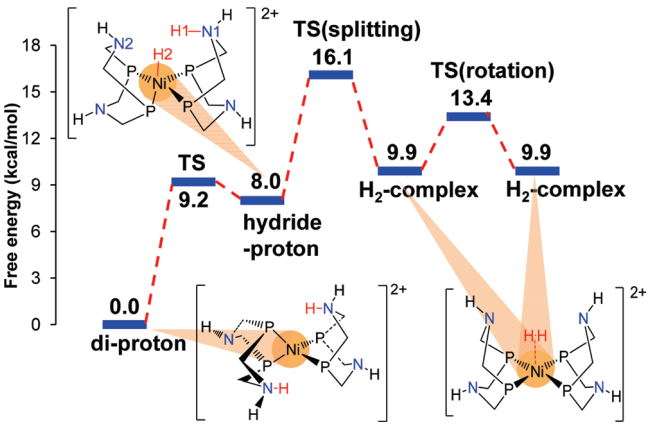

Figure 1. Calculated free-energy profile depicting (a) the H_2 rotation in the H_2-adduct (right-hand side), (b) the heterolytic cleavage of H_2 (middle), and (c) the hydride−proton to diproton rearrangement (left-hand side).

COMPUTATIONAL DETAILS

We carried out calculations on Vetere's model system, denoted $Ni(P_2^HN_2^H)_2$, in the boat−boat−chair−chair (bbcc) conformation, the exact same as Vetere's model. See ref 9 for discussion. All structures were optimized at the density functional theory (DFT) level of theory with the PBE[10,11] functional of the density and a mixed basis set which was comprised of the Stuttgart−Dresden relativistic ECP basis set (SDD)[12] for Ni and the 6-31G** basis set for all nonmetal atoms. Harmonic vibrational frequencies were calculated at the optimized structures using the same level of theory to estimate the zero-point energy (ZPE) and thermal contributions (298 K and 1 atm) to the gas-phase free energy. Free energies of solvation were then computed using a self-consistent reaction field (SCRF) model at the same level of theory as that for the other steps. The continuum polarizable conductor model (CPCM)[13,14] was used with Bondi radii.[15] All the calculations were carried out with Gaussian 09.[16] We did not have access to the software (ADF) used by these authors and were unable to reproduce their calculations exactly. Apart from numerical differences in the algorithms used by Gaussian 09 code and ADF, the only notable difference lies in the basis set. In a recent publication on a more realistic structural model,[8] we showed that the basis set employed here gave a very good description of the H_2 chemistry, both in terms of structures and energetics.

RESULTS

A free-energy diagram is displayed in Figure 1. From left to right, it includes several elementary steps: (a) starting from a diproton state (ΔG = +0.0 kcal/mol), the system evolves to a hydride−proton state (ΔG = +8.0 kcal/mol), passing through a transition state denoted as TS ($\Delta G^{\ddagger}$ = +9.2 kcal/mol); (b) from the hydride−proton state, the system evolves to a dihydrogen adduct (ΔG = +9.9 kcal/mol), passing through a heterolytic transition state denoted as TS(splitting) ($\Delta G^{\ddagger}$ = +16.1 kcal/mol); the dihydrogen adduct undergoes rotation along a C_2 axis, passing through the Ni atom and the midpoint of the H_2 molecule in the H_2 adduct. The transition state for this rotation is denoted TS(rotation). The H_2 molecule is weakly bound to the Ni(II) site in the H_2-adduct species. The coordinates for all of the species can be found in the Supporting Information. The important bond distances are gathered in Table 1. The structures and relative energies calculated here are closely consistent with those by Vetere et al.[5] Figure 1 shows that the H_2 molecule in the H_2-adduct can undergo rotation quite easily, with a barrier of

Table 1. Key Distances in Å in the Intermediates for H_2 Oxidation by $Ni(P_2^HN_2^H)_2^{2+}$

	H_2-adduct state	TS(rotation)	TS(splitting)	hydride−proton state	TS	diproton state
H1−H2	0.797	0.781	1.020	1.784	2.226	3.989
Ni−H2	1.933	1.898	1.640	1.509	1.493	2.450
N1−H1	2.302	2.920	1.374	1.060	1.063	1.062

dx.doi.org/10.1021/jp111479z |J. Phys. Chem. A 2011, 115, 4861–4865

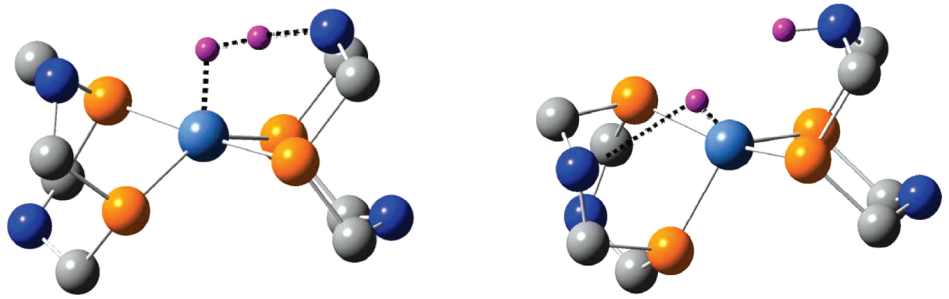

Figure 2. Structure of the transition state for heterolytic splitting of H_2 by $Ni(P_2^HN_2^H)_2^{2+}$ (left) and of the transition state for proton rearrangement from the proton−hydride species to the diproton species (right). All H atoms are removed for simplicity except those from the reactant H_2. The color code is Ni (light blue), P (orange), N (dark blue), C (gray), and H (purple).

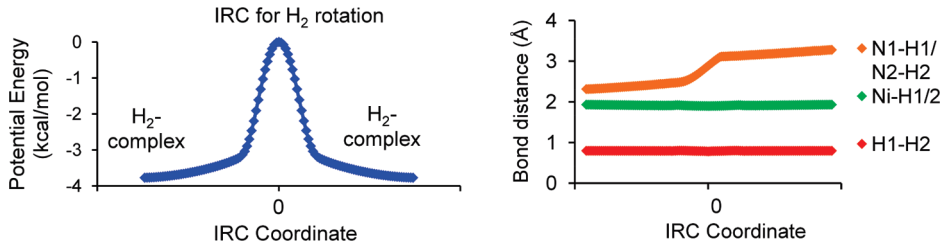

Figure 3. IRC energy profile for the rotation of the H_2 molecule around the C_2 axis in the H^2-adduct (left) and selected bond distances along the IRC coordinate (right).

3.5 kcal/mol. The structure labeled TS(rotation) is Vetere's transition state. The system has a C_2 axis of symmetry passing through the Ni atom and bisecting H_2 in this stable intermediate, in the transition state, and all along the pathway of rotation. The imaginary frequency at the TS(rotation) was found to be 448i cm^{-1}, a value in accord with Vetere's reported frequency.

In the H_2-adduct structure, the hydrogen atoms are far from the pendant amines, suggesting a nearly free rotation. The magnitude of the barrier to H_2 rotation (3.5 kcal/mol) can be rationalized on the basis of electrostatic arguments. The H_2-adduct structure is a dication, with the Ni atom in a (II) oxidation state and a d^8 electronic configuration. As a Lewis acid, the Ni(II) site creates an attractive electrostatic potential acting on the H_2 molecule and that polarizes the electron density of H_2 away from the H−H bond and toward the Ni(II) atom. The polarization of the electron density gives rise to small positive charges δ^+ on the H atoms that interact with the electron lone pairs of the two pendant amines. In the H_2-adduct complex, the interaction between the H atoms of H_2 and the pendant amines is thus electrostatic in nature and results in 3.5 kcal/mol needed to break this interaction all the way up to the transition state to rotation.

The center region of Figure 1 shows a path connecting the H_2-adduct structure to a hydride−proton structure with a hydridic hydrogen on Ni and a proton on a pendant amine. For this elementary step, the transition state labeled TS(splitting) is asymmetric. It lies 6.2 kcal/mol higher than the H_2-adduct. The imaginary frequency at the TS(splitting) is 755i cm^{-1}. The hydride−proton species lies 8.1 kcal/mol below the TS(splitting) transition state. On the left side of Figure 1, the hydride−proton state rearranges into a diproton state with two protons on two pendant amines. The diproton species is shown to lie 8.0 kcal/mol below the hydride−proton species. Stable diproton species of this type have been characterized spectroscopically.[5] The transition state labeled TS for the rearrangement of the hydride−proton state into a diproton state is shown to lie 1.2 kcal/mol above the hydride−proton state. The imaginary frequency of the TS transition state is 199i cm^{-1}. Ball and stick structures of TS(splitting) and TS are also shown in Figure 2. The asymmetric interactions of the hydrogen atoms with N and Ni in TS(splitting) can be clearly seen on the left picture. The structure of the TS transition state between a hydride−proton state and a diproton state resembles the hydride−proton state. This is consistent with Hammond's postulate about the structure of a transition state. In the case at hand, TS is very close in energy to the hydride−proton state, and the elementary step is strongly exothermic, leading to an early transition state with a structure that resembles the "reactant", that is, the hydride−proton structure.

To confirm our assignment of the pathways, we determined the IRCs for all three elementary steps displayed in Figure 1. The IRC profiles are shown in Figures 3, 4, and 5, along with the evolution of key bond lengths along the respective IRCs.

The IRC for H_2 rotation is shown in Figure 3. Among the key bond lengths displayed, it is notable that the H−H distance remains essentially constant along the IRC, with only a small decrease at the TS (Table 1) (also observed in Vetere's calculations), consistent with the weakening of the $N^{\delta-}\cdots{}^{\delta+}H-H^{\delta+}\cdots{}^{\delta-}N$ interactions described earlier. In addition, the N−H distances are never in the range of usual $N-H^+$ bonds as they should be if the IRC were indicative of H_2 being formed directly from two protons on two amines.

The IRC for H_2 splitting is shown in Figure 4. It can be seen that in the H_2-adduct, the H1−H2 distance is short and becomes long in the product state (hydride−proton). N1−H1 starts as a very long bond in the H_2-adduct and ends up a short bond in the hydride−proton state, while Ni−H2 is long in the H_2-adduct and short in the hydride−proton state. All of these observations are consistent with this IRC corresponding to a splitting of H_2 starting from the H_2-adduct and ending in a hydride−proton state.

dx.doi.org/10.1021/jp111479z |J. Phys. Chem. A 2011, 115, 4861–4865

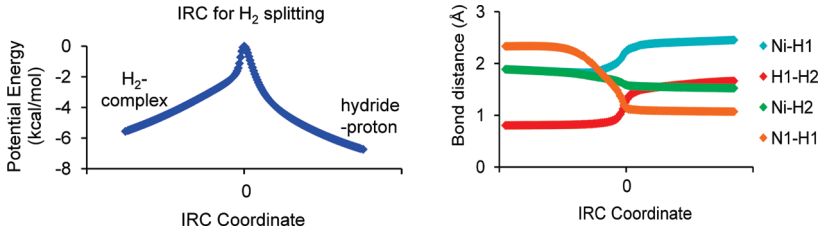

Figure 4. IRC energy profile for the heterolytic cleavage of H_2 connecting the H_2-adduct to a hydride−proton state (left) and selected bond distances along the IRC coordinate (right).

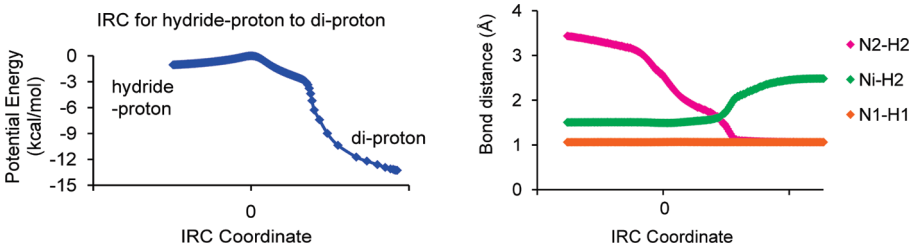

Figure 5. IRC energy profile for rearrangement of the proton connecting a hydride−proton state to a diproton state (left) and selected bond distances along the IRC coordinate (right).

The IRC for the hydride−proton to diproton rearrangement is displayed in Figure 5. The key distances show clearly that atom H2 transfers from Ni to atom N2, while atom H1 remains bound to N1 throughout the rearrangement.

CONCLUSIONS

In this Comment, we provided evidence that, contrary to a published interpretation of computational data, H_2 oxidation or proton reduction with the $Ni(P_2N_2)_2^{2+}$ family of electrocatalysts proceeds through a heterolytic cleavage or formation of the H_2 molecule between a H_2-adduct species and a hydride−proton species that can evolve further into a diproton species. All computational evidence points to a hydride−proton species being an intermediate. Characterization by NMR spectroscopy combined with molecular simulations of the collective dynamics in the intramolecular exchange process for these electrocatalysts strongly supports the existence of this intermediate.[17] Knowing and understanding the detailed mechanism of H_2 oxidation and H_2 evolution is critical for the further development of improved catalysts as it affects their rational design through matching of metal hydricities, pK_a's, redox potentials, and amine pK_a's.

ASSOCIATED CONTENT

Supporting Information. List of Cartesian coordinates. This material is available free of charge via the Internet at http://pubs.acs.org.

ACKNOWLEDGMENT

This research was carried out in the Center for Molecular Electrocatalysis, an Energy Frontier Research Center funded by the U.S. Department of Energy, Office of Science, Office of Basic Energy Sciences. Pacific Northwest National Laboratory is operated for the U.S. Department of Energy by Battelle under Contract No. DE-AC06-76RLO 1830. Computational resources were provided at W. R. Wiley Environmental Molecular Science Laboratory (EMSL), a national scientific user facility sponsored by the Department of Energy's Office of Biological and Environmental Research located at Pacific Northwest National Laboratory and the National Energy Research Scientific Computing Center (NERSC) at Lawrence Berkeley National Laboratory.

REFERENCES

(1) *Catalysis Without Precious Metals*; Bullock, R. M., Ed.; Wiley-VCH: Weinheim, Germany, 2010.
(2) Rakowski DuBois, M.; DuBois, D. L. *Acc. Chem. Res.* **2009**, *42*, 1974.
(3) Rakowski DuBois, M.; DuBois, D. L. *Chem. Soc. Rev.* **2009**, *38*, 62.
(4) Wilson, A. D.; Newell, R. H.; McNevin, M. J.; Muckerman, J. T.; Rakowski DuBois, M.; DuBois, D. L. *J. Am. Chem. Soc.* **2006**, *128*, 358.
(5) Wilson, A. D.; Shoemaker, R. K.; Miedaner, A.; Muckerman, J. T.; DuBois, D. L.; DuBois, M. R. *Proc. Natl. Acad. Sci. U.S.A.* **2007**, *104*, 6951.
(6) Yang, J. Y.; Bullock, R. M.; Shaw, W. J.; Twamley, B.; Fraze, K.; DuBois, M. R.; DuBois, D. L. *J. Am. Chem. Soc.* **2009**, *131*, 5935.
(7) Yang, J. Y.; Chen, S.; Dougherty, W. G.; Kassel, W. S.; Bullock, R. M.; DuBois, D. L.; Raugei, S.; Rousseau, R.; Dupuis, M.; Rakowski DuBois, M. *Chem. Commun.* **2010**, *46*, 8618.
(8) Chen, S.; Raugei, S.; Rousseau, R.; Dupuis, M.; Bullock, R. M. *J. Phys. Chem. A* **2010**, *114*, 12716.
(9) Kachmar, A.; Vetere, V.; Maldivi, P.; Franco, A. A. *J. Phys. Chem. A* **2010**, *114*, 11861–11867.
(10) Perdew, J. P.; Burke, K.; Ernzerhof, M. *Phys. Rev. Lett.* **1996**, *77*, 3865.
(11) Perdew, J. P.; Burke, K.; Ernzerhof, M. *Phys. Rev. Lett.* **1997**, *78*, 1396.
(12) Andrae, D.; Häussermann, U.; Dolg, M.; Stoll, H.; Preuss, H. *Theor. Chem. Acc.* **1990**, *77*, 123.
(13) Barone, V.; Cossi, M. *J. Phys. Chem. A* **1998**, *102*, 1995.
(14) Cossi, M.; Rega, N.; Scalmani, G.; Barone, V. *J. Comput. Chem.* **2003**, *24*, 669.
(15) Bondi, A. *J. Phys. Chem.* **1964**, *68*, 441–451.
(16) Frisch, M. J.; Trucks, G. W.; Schlegel, H. B.; Scuseria, G. E.; Robb, M. A.; Cheeseman, J. R.; Scalmani, G.; Barone, V.; Mennucci, B.; Petersson, G. A.; Nakatsuji, H.; Caricato, M.; Li, X.; Hratchian, H. P.; Izmaylov, A. F.; Bloino, J.; Zheng, G.; Sonnenberg, J. L.; Hada, M.;

Ehara, M.; Toyota, K.; Fukuda, R.; Hasegawa, J.; Ishida, M.; Nakajima, T.; Honda, Y.; Kitao, O.; Nakai, H.; Vreven, T.; Montgomery, J. A., Jr.; Peralta, J. E.; Ogliaro, F.; Bearpark, M.; Heyd, J. J.; Brothers, E.; Kudin, K. N.; Staroverov, V. N.; Kobayashi, R.; Normand, J.; Raghavachari, K.; Rendell, A.; Burant, J. C.; Iyengar, S. S.; Tomasi, J.; Cossi, M.; Rega, N.; Millam, J. M.; Klene, M.; Knox, J. E.; Cross, J. B.; Bakken, V.; Adamo, C.; Jaramillo, J.; Gomperts, R.; Stratmann, R. E.; Yazyev, O.; Austin, A. J.; Cammi, R.; Pomelli, C.; Ochterski, J. W.; Martin, R. L.; Morokuma, K.; Zakrzewski, V. G.; Voth, G. A.; Salvador, P.; Dannenberg, J. J.; Dapprich, S.; Daniels, A. D.; Farkas, O.; Foresman, J. B.; Ortiz, J. V.; Cioslowski, J.; Fox, D. J. *Gaussian 09*; Gaussian, Inc.: Wallingford CT, 2009.

(17) O'Hagan, M.; Shaw, W.; Raugei, S., Chen, S.; Yang J. Y.; Kilgore U. J.; DuBois, D. L.; Bullock R. M. In preparation.